1 **Biomechanical, ultrastructural, and electrophysiological characterization of the non-**
2 **human primate experimental glaucoma model**
3

4 **Authors:** VijayKrishna Raghunathan[1,2,3,#], J. Seth Eaton[1,2,#], Brian J. Christian[4], Joshua T.
5 Morgan[1], James N. Ver Hoeve[2,5], Chen-Yuan Charlie Yang[6,7], Haiyan Gong[6,7], Carol A.
6 Rasmussen[2,5], Paul E. Miller[2,8], Paul Russell[1,2], *T. Michael Nork[2,5], *Christopher J.
7 Murphy[1,2,9]
8

9 **Affiliations:** [1]Department of Surgical and Radiological Sciences, School of Veterinary
10 Medicine, University of California – Davis, Davis, California, 95616
11 [2]Ocular Services On Demand (OSOD), Madison, Wisconsin 53719
12 [3]The Ocular Surface Institute, Department of Basic Sciences, College of Optometry,
13 University of Houston, Houston, Texas, 77204
14 [4]Covance Laboratories, Inc., Madison, Wisconsin 53704
15 [5]Department of Ophthalmology and Visual Sciences, School of Medicine and Public
16 Health, University of Wisconsin – Madison, Madison, Wisconsin 53792
17 [6]Department of Anatomy and Neurobiology, School of Medicine, Boston University,
18 Boston, Massachusetts 02118
19 [7]Department of Ophthalmology, School of Medicine, Boston University, Boston,
20 Massachusetts 02118
21 [8]Department of Surgical Sciences, School of Veterinary Medicine, University of
22 Wisconsin – Madison, Madison, Wisconsin 53706
23 [9]Department of Ophthalmology & Vision Science, School of Medicine, University of
24 California – Davis, Sacramento, California 95817
25

26 [#] contributed equally to the work presented here and should therefore be regarded as
27 equivalent authors
28

29 **Co-Corresponding Authors:**

|	
T. Michael Nork, MD, MS	Christopher J. Murphy, DVM, PhD, DACVO
Department of Ophthalmology and Visual Sciences	
University of Wisconsin Medical School	School of Veterinary Medicine
600 Highland Ave, K6/456	University of California – Davis
Madison, WI 53792-4673	1 Shields Avenue
tmnork@wisc.edu	1423 Tupper Hall
	Davis, CA 95616
	cjmurphy@ucdavis.edu

30

31

32 **SUPPLEMENTAL FIGURES**

33 **Fig S1.** Scatterplots (see **Fig. 2** for details) for a- and b-waves from 2.5, 4.0 and 14.0 cd-s

34 m-2 flash intensities recorded under light adapted (top row) and dark adapted (bottom row)

35 conditions. Although there are significant differences between control (blue triangle) and

36 ExGl (red circles) eyes, there is no consistent evidence of a correlation between these

37 measures and loss of nerve fiber layer thickness. Similar results were found for 30 Hz

38 flicker (not shown).
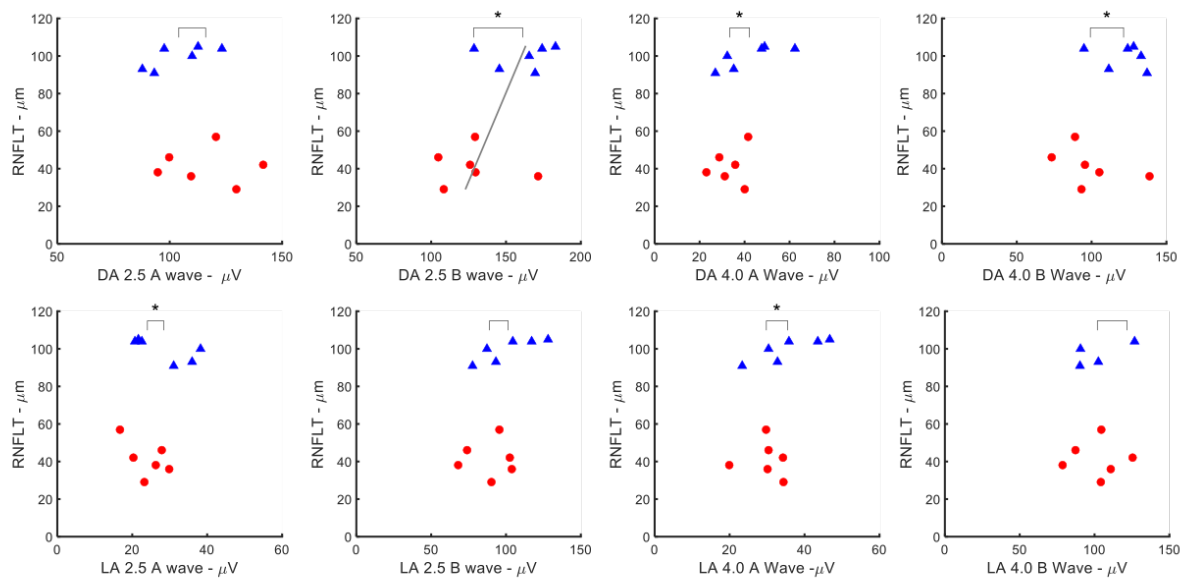
39

40

41   **Fig S2.** Histogram representing the elastic moduli of TM with respect to difference in

42   intraocular pressure (IOP) at the time of euthanasia in individual animals between normal

43   eyes (blue) and eyes with ExGl (red).
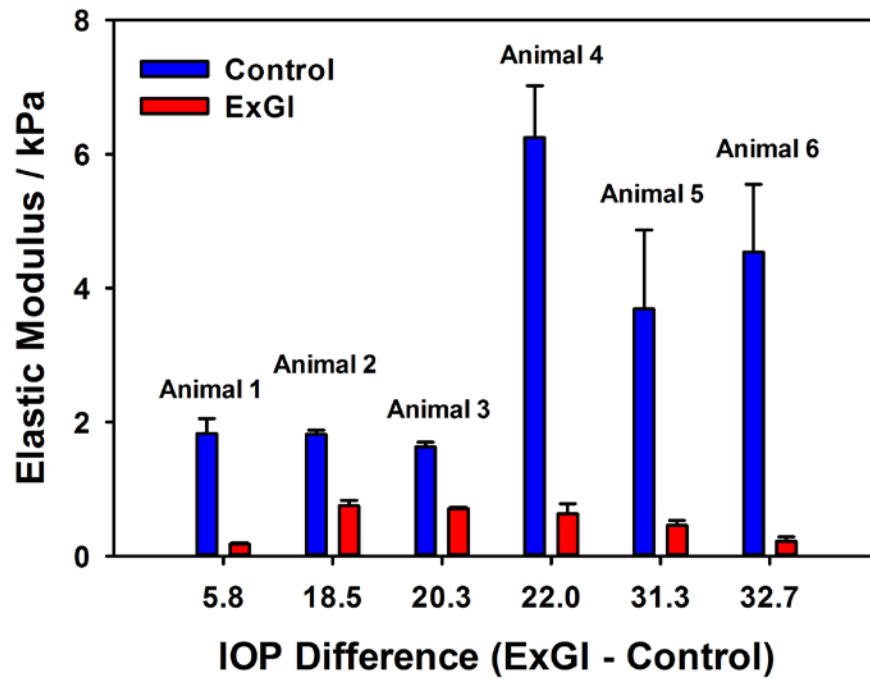
44

45   **Fig S3.** Principal component analysis plots: scree plot identifying the number of principal

46   components that define the proportion of variance in data is illustrated. Plot of PC1 versus

47   PC2 demonstrates data clustering for Control (OS) vs ExGl (OD) tissue samples.
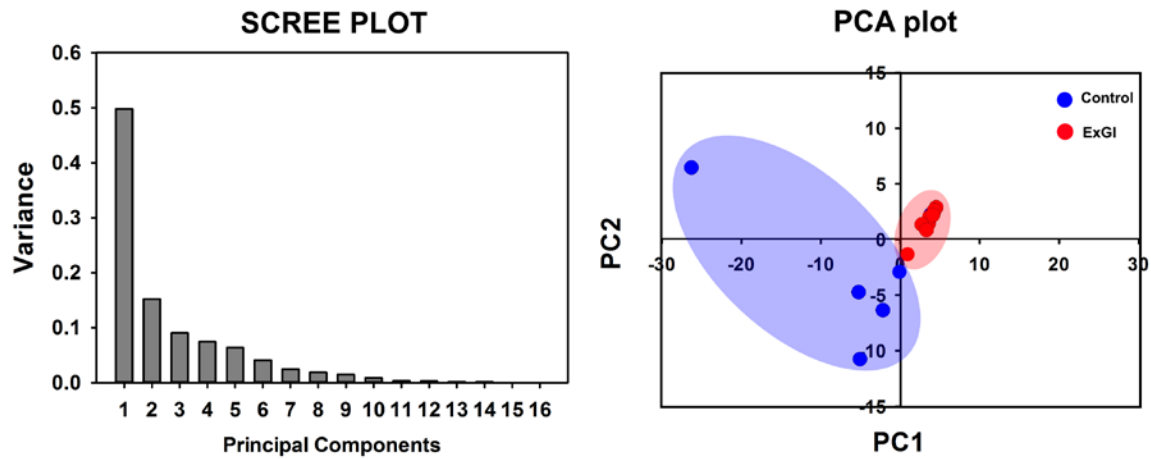
48

49   **Fig S4.** Global image of the fluorescent tracers in the trabecular meshwork (TM) in eyes

50   of monkeys with EG (hypertensive) and fellow untreated controls (normal). The tracers'

51   distribution in the TM (posterior view of the eye) from all three pairs of eyes is shown,

52   which served as guides for later dissection of the hypertensive eyes to correspond non-

53   lasered regions, where tracers were often observed and lasered regions where tracers were

54   mostly not observed.

55
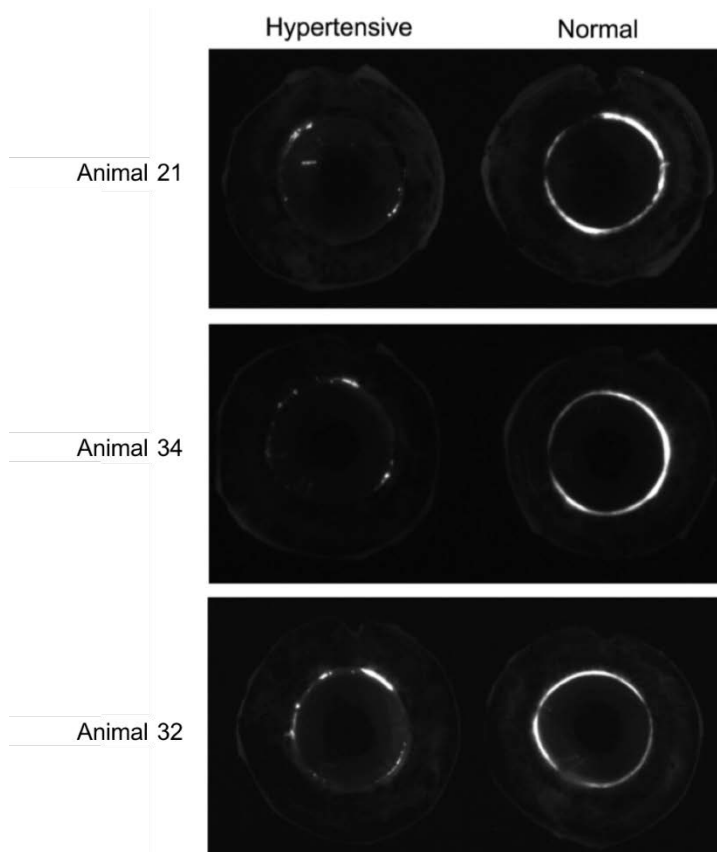
56

57

58 **MATERIALS & METHODS**

59 **Animals**

60 Thirty-two eyes of 16 adult female cynomolgus macaques (*Macaca fascicularis*) were

61 analyzed in the course of this study. All experimental methods and procedures were

62 approved by the Animal Care and Use Committee at Covance Laboratories, Inc. (Madison,

63 WI), and were performed consistent with the ARVO Statement for the Use of Animals in

64 Ophthalmic and Vision Research. At least 3 years prior to euthanasia and collection of

65 globes, all animals had undergone unilateral laser trabeculoplasty (right eye [OD] only) to

66 induce ExGl. Prior to euthanasia and inclusion in the present study, all animals had been

67 used in preclinical investigations evaluating the hypotensive efficacy of topical test

68 substances. The identities and properties of these test substances are proprietary and cannot

69 be disclosed. To avoid the potentially confounding effect of day-to-day IOP fluctuations in

70 this model[52], treatment periods with any substance were typically short in duration (<48

71 hours), or involved administration of only a single topical drop applied followed by a 2-

72 week monitoring period. This also mitigated possibly confounding long-term effects on the

73 TM. Furthermore, all animals had undergone washout periods without any topical

74 medications prior to euthanasia. The inclusion criteria (age, duration between onset of

75 glaucoma and euthanasia, and washout period) for all animals, designated as Sets A-C, are

76 presented in **Table 1**. All *in vivo* and *ex vivo* measurements and procedures performed for

77 these animals are summarized in **Table 2**. Whole globes from Set A animals were

78 submitted for confocal, light, and transmission electron microscopy (TEM); corneoscleral

79 rims from Set B and C animals were submitted for proteomic analysis and/or atomic force

80 microscopy (AFM).

81 **Laser Trabeculoplasty Procedure and Establishment of Experimental Glaucoma**

82 **(ExGl)**

83 All laser trabeculoplasty procedures were performed by a board-certified veterinary

84 ophthalmologist with extensive experience in comparative glaucoma research. Animals

85 were anesthetized with ketamine (10 mg/kg IM) and xylazine (0.5 mg/kg IM), or ketamine

86 (10 mg/kg IM) and dexmedetomidine (0.025 mg/kg IM). In animals receiving

87 dexmedetomidine, anesthesia was reversed with atipamezole (0.25 mg/kg IM). A 532 nm

88 diode laser (Oculight™ GL Diode Laser, Iridex Corp., Mountain View, CA) and a

89 Kaufman Single Mirror Laser Lens specifically designed for NHPs (Ocular Instruments,

90 Inc.™, Bellevue, WA) were used to ablate the majority (approximately 11 clock-hours) of

91 the trabecular meshwork (TM) of all right eyes to induce unilateral ExGl. The initial

92 procedure treated the inferior 180° of the TM, using a contiguous series of laser burns with

93 a spot size of 75 microns (the smallest size for this laser) at an initial power of 1 W for 0.5

94 seconds. Treatment was focused on the non-pigmented portion of the TM, as contiguous

95 treatment in the often heavily pigmented TM of cynomolgus macaques can result in a

96 cyclodialysis cleft and permanent hypotony. This did not occur in any eyes used in this

97 study. The amount of applied laser energy was adjusted to result in whitening or bubble

98 formation of the TM without inducing hemorrhage. The second procedure used an identical

99 approach to treat the superior 180°, except for up to approximately 1 clock-hour of TM.

100 The anatomical location of the unlasered TM was recorded by the surgeon. The last

101 treatment was performed a minimum of 3 years before euthanasia. All contralateral left

102 eyes (OS) served as untreated normotensive controls.

103 Slit-lamp biomicroscopy and indirect ophthalmoscopy were regularly performed following

104 laser treatments, and all observations were quantified using a modified McDonald-

105 Shadduck clinical scoring system [53]. In all animals, postoperative aqueous flare and cells

106 were transiently observed but did not persist clinically. Topical atropine was administered

107 postoperatively to control iridocyclospasm, but topical steroids were not administered as

108 to encourage fibrosis of the laser-treated TM. Intraocular pressure (IOP) was periodically

109 measured using a Model 30 Classic Pneumotonometer (Medtronic Solan™, Jacksonville,

110 FL) after corneal anesthesia (**Table 2**). All animals were trained to accept IOP

111 measurements without sedation. The only exception was the IOP measurement just prior

112 to sacrifice during which the animals were lightly sedated with ketamine. In NHPs,

113 however, there is evidence that ketamine alone does not lower IOP unless it is given

114 multiple times over multiple consecutive days [54]. It is noteworthy that 4 animals whose

115 globes were processed for AFM required periodic topical treatment with levobunolol to

116 control excessively high IOP (> 55 mmHg) in the year prior to euthanasia. We do not,

117 however, believe this to have significantly confounded our data.

118 **Spectral-Domain Optical Coherence Tomography (SD-OCT)**

119 Spectral-domain optical coherence tomography (SD-OCT) scans of the fundus were

120 carried out in both eyes of all animals using a Heidelberg™ Spectralis HRA+OCT

121 (Heidelberg Engineering, Heidelberg, Germany) instrument prior to euthanasia. Animals

122 were anesthetized with ketamine (10 mg/kg IM), oxymorphone (0.15 mg/kg), and

123 dexmedetomidine (0.025 mg/kg IM). Anesthesia was reversed with atipamezole (0.25

124 mg/kg) and naloxone (0.2 mg/kg). Set A animals (N=3) were scanned twice, once with

125 both the Spectralis and a Zeiss™ Cirrus HD-OCT 4000 (Carl Zeiss, Oberkochen,

126 Germany) on the same day, and again 8 months later with the Spectralis. For all animals

127 (N=16), the following were collected: macular scans (Heidelberg macular volume / Cirrus

128 macular cube), high resolution line scans through the macula, high resolution line scans

129 through the optic nerve, and retinal nerve fiber layer (RNFL) scans (Heidelberg glaucoma

130 circle / Cirrus optic nerve cube). Evaluation of scans focused on the RNFL, retinal ganglion

131 cell layer (RNGL), optic nerve head (ONH), and macula. Segmentation and determination

132 of RNFL thickness (RNFLT) was performed using standard automated algorithms as well

133 as manual and combined (EdgeSelect™) techniques [55].

134 **Electrodiagnostics**

135 All animals were anesthetized for electrodiagnostics. For ffERG and VEP, animals were

136 anesthetized with ketamine (10 mg/kg IM) and dexmedetomidine (0.025 mg/kg IM); and

137 anesthesia was reversed with atipamezole (0.25 mg/kg). For PERG, animals were

138 anesthetized with ketamine (10 mg/kg IM), oxymorphone (0.15 mg/kg), and

139 dexmedetomidine (0.025 mg/kg IM); and anesthesia was reversed with atipamezole (0.25

140 mg/kg) and naloxone (0.2 mg/kg).

141   In Set B animals (N=6), photopic and scotopic full-field ERGs (ffERG) to a series of

142 flash strengths, photopic flash visual-evoked potentials (fVEP), pattern electroretinograms

143 (PERG) and pattern reversal visual evoked potentials (PRVEP) were recorded in two

144 sessions using a BigShot™ electrodiagnostic system (LKC Technologies™, Gaithersburg,

145 MD).

146   Following a minimum of 2 h of dark adaptation, animals were routinely anesthetized

147 and pupils were dilated with 1% tropicamide and 2.5% phenylephrine hydrochloride.

148 Corneas were anesthetized with topical 0.5% proparacaine prior to application of ERG-

149 jet™ (Universo,™, Switzerland) contact lens electrodes and a conductive wetting solution.

150 Reference electrodes were subdermal stainless steel needle electrodes inserted near the

151 ipsilateral outer canthus of each eye. Visual evoked potentials were recorded from two

152 active stainless steel subdermal electrodes situated approximately 1 cm superior to the

153 occipital ridge and 1 cm lateral to the midline; VEP reference electrodes were situated

154 adjacent to one another along the midline at the vertex. Dark-adapted ERGs were recorded,

155 followed by 10 min of light adaptation, followed by the light-adapted series. Following

156 full-field ERG testing, flash-evoked VEPs and PERGs and PRVEPs were recorded. For

157 pattern stimulation recordings, animals were refracted for the viewing distance of 30 cm.

158   ERG and VEP waveforms were processed off-line and machine scored using software

159 written in Matlab™ (Nattick, MA). Oscillatory potentials (OPs) were derived from the 2.5

160 cd-s m-2 flash conditions and bandpass filtered between 70 and 170 Hz. OPs and flash

161 VEPs were quantified as the root-mean-square of the response from 10-160 msec post

162 flash.

163 **Collection and Fixation of Globes**

164 Following euthanasia, all eyes were immediately enucleated and all right eyes with ExGl

165 were marked to facilitate identification of the unlasered area of the TM. For AFM and

166 proteomics (Sets B and C), corneoscleral rims were dissected, placed in Optisol™ and

167 refrigerated before shipping from Covance Laboratories to the University of California –

168 Davis. For confocal and light microscopy and TEM (Set A), whole globes were similarly

169 enucleated and refrigerated, each placed in a moist container, and shipped refrigerated to

170 Boston University within 24 hours of euthanasia.

171 **Atomic Force Microscopy (AFM)**

172   Within 24 h post-euthansia, tissue samples were received at UC Davis for AFM analysis.

173   After receipt, the unlasered portion of TM from right eyes (OD) with ExGl (Sets B and C)

174   was microdissected according to data from the surgeon's records, and the corresponding

175   marking designated at enucleation. The elastic modulus determined using AFM according

176   to methods previously described for human TM [13,42,56]. A similar dissection was done for

177   the normal left eyes (OS) and AFM performed using a portion of TM of approximately the

178   same size as the samples from eyes with ExGl. Briefly, all force vs. indentation curves

179   were obtained, with the TM tissue placed in Hank's Balanced Salt Solution (HBSS), using

180   the MFP-3D BIO system (Asylum Research™, Santa Barbara, CA). Force curves (5 per

181   location) were obtained from 5 random locations along the length of the tissue. All force

182   curves were obtained within 1 h of dissection to mitigate effects from any inadvertent

183   degradation of tissues.

184   **Proteomics**

185   Within 24 h post-euthansia, tissue samples were received at UC Davis for proteomic

186   analysis. Unlasered TM tissue was microdissected from ExGl eyes and controls using the

187   technique described above. Isolated tissue samples were immediately digested in RIPA

188   buffer, homogenized, and stored at -80°C until analysis. Samples were precipitated and

189   analyzed as described previously [42,57]. Mass spectra were collected in a data-dependent

190   mode. Peptide fragmentation was performed using higher-energy collision dissociation

191   (HCD) with a normalized collision energy (NCE) value of 27. Unassigned charge states as

192   well as +1 and ions >+5 were excluded from MS/MS fragmentation. Tandem mass spectra

193   were extracted and charge states were deconvoluted and deisotoped. All MS/MS samples

194   were analyzed using X! Tandem (The GPM, thegpm.org; version X! Tandem

195   Sledgehammer (2013.09.01.1)). X! Tandem was set up to search the Uniprot Macaca

196   fascicularis (29,946 entries) plus an equal number of reverse sequences and 60 common

197   non-human laboratory contaminant proteins, assuming the digestion was enzymatic using

198   trypsin. X! Tandem was searched with a fragment ion mass tolerance of 20 PPM and a

199   parent ion tolerance of 20 PPM. Carbamidomethyl of cysteine was specified in X! Tandem

200   as a fixed modification. Glu->pyro-Glu of the N-terminus, ammonia-loss of the N-

201   terminus, gln->pyro-Glu of the N-terminus, deamidated of asparagine and glutamine,

202   oxidation of methionine and tryptophan, and dioxidation of methionine and tryptophan

203   were specified in X! Tandem as variable modifications. Scaffold™ (version

204   Scaffold_4.3.0, Proteome Software Inc., Portland, OR, USA) was used to validate MS/MS-

205   based peptide and protein identifications. Peptide identifications were accepted if they

206   could be established at a 99.0% probability by the Scaffold Local FDR algorithm; this

207   corresponded to a 0.22% spectra decoy FDR and a 4% protein decoy FDR with 1 identified

208   peptide per protein. Protein probabilities were assigned by the Protein Prophen algorithm

209   13. Proteins that contained similar peptides and could not be differentiated based on

210   MS/MS analysis alone were grouped to satisfy the principles of parsimony. Proteins

211   sharing significant peptide homology were grouped into clusters.

212   **Confocal, Light Microscopy (LM) and Transmission Electron Microscopy (TEM)**

213   **Morphology**

214   Immediately following enucleation, both eyes from Set A animals were refrigerated and

215   shipped to Boston University for ocular perfusion, confocal, light microscopy (LM), and

216   TEM of TM from both untreated eyes, and the non-lasered regions of eyes with ExGl. The

217 last measurement of IOPs on the day of sacrifice were used for the analysis and to set the

218 subsequent perfusion pressure.

219 *Ex vivo ocular perfusion*

220 Enucleated eyes were perfused with Dulbecco's phosphate-buffered saline containing 5.5

221 mM D-glucose (GPBS) with the perfusion pressure set at the pre-mortem intraocular

222 pressure minus 7 mmHg (episcleral venous pressure) for 15-30 minutes. This time was set

223 based on previous reports for establishing a stable outflow facility [8]. A previously

224 established two-color fluorescent tracer method [58] was used to label the aqueous outflow

225 patterns (green or red tracers; 500 or 200 nm; 0.002%). The anterior chamber contents were

226 exchanged prior to perfusion with the same perfusates (tracers, GPBS, and fixative). All

227 eyes were perfused with a fixed volume. Eyes were perfusion-fixed with modified

228 Karnovsky's fixative and immersed-fixed overnight with the same fixative before further

229 processing.

230 *Fluorescent tracer distribution in the TM and TM thickness by confocal microscopy*

231 The eyes were hemisected along the equator, and the vitreous humor, ciliary body and lens

232 were removed. Tracer distribution from the TM sides of the anterior chamber was imaged

233 by a global imaging technique [59] using a 300mm lens on a 4000MP VersaDoc™ imaging

234 system (Bio-Rad Laboratories, Hercules, CA). The tracer distributions from the TM served

235 as guides for later dissection of the hypertensive eyes correlating to non-lasered regions

236 where tracers were observed, and lasered regions where tracers were not observed (**Fig.**

237 **S4**). The anterior segments of the eyes were further divided into smaller wedges. For

238 normal control eyes, tissue regions similar to the non-lasered regions of hypertensive eyes

239 were used to analyze the TM thickness with confocal microscopy (Carl Zeiss 510,

240 Axiover™ 200M Laser Scanning Microscope, Carl Zeiss) and the Schlemm's canal /

241 juxtacanalicular tissue (SC/JCT) regions with electron microscopy. Each confocal image

242 was measured at two to three different locations for TM thickness (the length from the

243 innermost uveoscleral beam to the inner wall endothelium of SC), and the average

244 thickness of TM in high-tracer regions of the hypertensive and normal control eyes were

245 then calculated and analyzed.

246 *Giant vacuoles density and ultrastructure of the inner wall of Schlemm's canal and*

247 *juxtacanalicular tissue*

248 After confocal imaging, frontal tissue sections were post-fixed in 2% osmium tetroxide,

249 1.5% potassium ferrocyanide in water for 2 hours, followed by *en bloc* staining with uranyl

250 acetate, dehydrated in an ascending series of ethanol, infiltrated with propylene aside and

251 embedded in Epon-Araldite. Semi-thin sections were cut and stained with 1% Toluidine

252 Blue (Fisher Scientific, Pittsburgh, PA). Light micrographs along the inner wall of the SC

253 were taken using the Olympus™ FSX100 imaging system with a 40X objective. The

254 number of giant vacuoles was counted along the inner wall of SC where the SC was open.

255 Ultra-thin sections were cut and the ultrastructure of the inner wall of SC and JCT regions

256 were examined with a transmission electron microscope (JOEL™ JEM-1011, Tokyo,

257 Japan). The percentage of SC length missing inner wall cells was then measured from the

258 electron micrographs.

259 **Statistical analysis**

260 Differences in ERG parameters were evaluated by paired-sample t-tests. Correlation with

261 SD-OCT RNFL thickness was assessed with non-parametric Spearman's rho coefficient.

262 For AFM measurements, elastic modulus was represented as either box plots or bar charts

263   (mean ± standard error in mean) from both eyes. Statistical significance was determined

264   by performing unpaired Student's t-test between the two groups for each animal (*p<0.05,

265   **p<0.01, ***p<0.001). To ascertain quantitative differences in biochemical composition

266   of the TM derived from the lasered and unlasered eyes, nano-scale liquid chromatography

267   tandem-mass spectrometry was performed. Proteomics data were analyzed using the built-

268   in features of Scaffold viewer (Proteome Software Inc., OR). Normalized total spectral

269   counts from the TM samples were compared for fold-change between the OS and OD eyes.

270   Fisher's exact test was performed to account for relative abundance in proteins between

271   the groups. For morphological analysis, unpaired two-tailed Student's t-test was used for

272   statistical analysis; results are shown as mean ± standard deviation (SD).

273